Journal of Power Sources 196 (2011) 1677–1686

Contents lists available at ScienceDirect

Journal of Power Sources

journal homepage: www.elsevier.com/locate/jpowsour

Review

Micro-tubular solid oxide fuel cells and stacks

Katie S. Howe*, Gareth J. Thompson, Kevin Kendall

SOFC Research Group, Centre for Hydrogen and Fuel Cell Research, University of Birmingham, Birmingham B15 2TT, UK

ARTICLE INFO

Article history:
Received 8 June 2010
Received in revised form
13 September 2010
Accepted 21 September 2010
Available online 1 October 2010

Keywords:
Tubular solid oxide fuel cell
Micro-SOFC
Stack
Performance

ABSTRACT

The properties and performance of micro-tubular solid oxide fuel cells are compared and the differentiating factors discussed. The best recorded power density for a single cell in the literature to date is 1.1 W cm^{-2}, with anode microstructure and current collection technique emerging as two key factors influencing electrical performance. The use of hydrocarbon fuels instead of pure hydrogen and methods for reducing the resultant carbon deposition are briefly discussed. Performance on thermal and reduction–oxidation (RedOx) cycling is also a critical issue for cell durability. Combining these individual cells into stacks is necessary to obtain useful power outputs. As such, issues of fluid and heat transfer within such stacks become critical, and computational modelling can therefore be a useful design tool. Experimentally tested stacks and stack models are discussed and the findings summarised. New results for a simple stack manufactured at the University of Birmingham are also given.

Contents

1. Introduction

Tubular solid oxide fuel cells (SOFCs) were pioneered in the 1960s [1,2], becoming commercially available in the 1970 s, when Westinghouse began to use an electrochemical vapour deposition technique for their fabrication [3,4]. This design reduced the problems of brittleness and sealing as compared to planar cells, but still required a heat up time of 4–6 h. Whilst their performance was good, with single cells exceeding 20,000 h of operation [5], they did not have a high power density (only around 0.6 W cm^{-3} [6]; around half that obtained for planar cells at the time). For tubular cells, power density depends upon the inverse of cell diameter; the narrower, the better the performance. This observation led to the invention of micro-tubular SOFCs (mSOFCs) by K. Kendall in

* Corresponding author. Tel.: +44 121 4145283; fax: +44 121 4145324.
E-mail address: kxh984@bham.ac.uk (K.S. Howe).

0378-7753/$ – see front matter © 2010 Elsevier B.V. All rights reserved.
doi:10.1016/j.jpowsour.2010.09.043

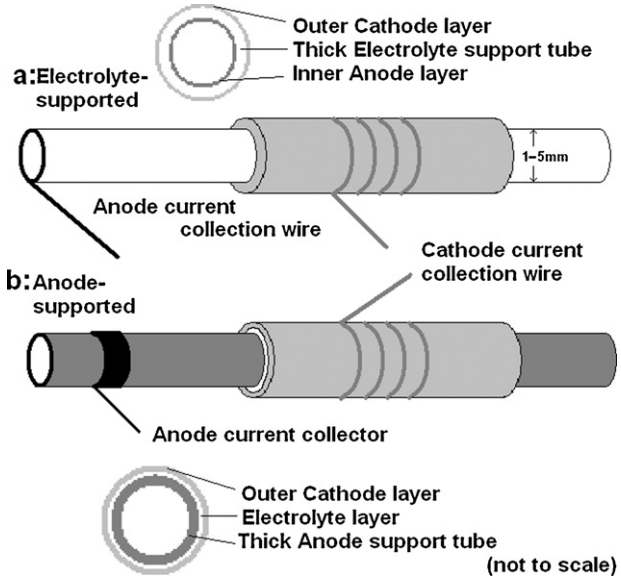

Fig. 1. Basic micro-tubular fuel cell designs.

the early 1990s [7] (early work by Kendall [8]), and the following review is focused on this design.

These tubes are on the scale of millimetres, unlike the tens of centimetres for their predecessors. mSOFCs have the advantage that they have short start–up times (on the order of a few seconds for a single cell), are resistant to thermal degradation on cycling and have high power densities (around 2.5 W cm^{-3} [9]) and less stringent sealing requirements than planar cells, where all four edges must be made gas tight. Interconnects and current collection do provide new problems, however, especially when assembling these into stacks. As such, there are still issues to be resolved. A comprehensive review comparing these micro-tubular cells to other SOFC designs has recently been presented by Kendall [10]. The purpose of this paper is to compare performances of different mSOFCs and review the progress that has been made since their inception.

In addition to the discussion of individual cells, progress in stack design is summarised. As each mSOFC tube only produces approximately half a Watt of electrical power, these must be combined into stacks of various sizes to meet application demands. Soon after Kendall's invention of micro-tubular fuel cells [7], he and his group demonstrated 200-cell [11] and 1000-cell [12] stacks. Since then, new stack and interconnect configurations have been designed and tested, as discussed below. Lower operating temperatures and higher power densities are the two main research targets.

2. mSOFC design

The first mSOFCs, made in the early 1990 s, were based on extruded tubes of yttria-stabilised zirconia (YSZ) [7] up to 5 mm in diameter, with wall thicknesses in the range of 100–200 μm. YSZ formed the electrolyte material, and anode and cathode layers were then added to this supporting electrolyte tube. A schematic of such an electrolyte-supported cell is shown in Fig. 1a.

Other designs of mSOFC have also been investigated with anode-supported cells (YSZ and nickel cermet anode tube—schematic in Fig. 1b) emerging as strong competitors for the original electrolyte-supported model [13]. The anode support allows for a thinner electrolyte (3–30 μm, the work of Tan et al. [14] having one of the thinnest), and therefore lower Ohmic resistance. Most recent mSOFC research has used anode-supported cells.

In both designs, the support tube is longer than the active cell length. The first tube segment provides a gas inlet tube and the outlet section can be used as a combustor tube, where the fuel (hydrogen, short-chain hydrocarbons, etc.) and oxidant (oxygen or air) combine. Cathode-supported designs have also been investigated [15,16], but are not common in the literature due to the high polarisation resistance [17,18] of the cathode tube weakening performance (Liu et al. reported a decrease of power density by over 60% when changing from an anode-supported cell to an otherwise similar cathode-supported cell [16,19]).

Co-extrusion to form multi-layer tubes has also been demonstrated [20]. This enables better matching of thermal expansion coefficients by increasing the number of steps from e.g. 100% YSZ (electrolyte) to the 90% nickel, 10% YSZ anode, reducing cracking on thermal cycling.

Table 1
"Traditional" materials for mSOFC components.

mSOFC component	Material used
Anode	YSZ and Nickel cermet (often with added pore-formers/dopants)
Electrolyte	Yttria-stabilised zirconia (YSZ, ~8–10 mole% yttria)
Cathode	Lanthanum strontium manganite (LSM) [LSM/YSZ more recently]
Anode current collector	Nickel
Cathode current collector	Silver

2.1. Materials used

"Traditional" materials used for each component of mSOFCs are listed in Table 1. These are by no means the only options, and some other choices will be discussed in more detail later. Jacobson [21] discusses these materials in some detail, focusing on those suitable for lower operating temperatures. The required properties for the electrolyte and electrodes are briefly described below. Whilst material choices are briefly discussed here, materials and manufacture are not considered in detail. These two issues are covered more fully by Mizutani's review [22], which focuses on Japanese research and development.

The electrolyte: The two main requirements for the mSOFC electrolyte material are:

- Pure ionic conductivity
- Stability

The theoretical operation of a SOFC requires transport of oxygen ions (O^{2-} anions) only through the electrolyte. Passage of electrons, or hydrogen ions (H^+ cations), through this material would result in short circuiting or combustion, respectively. In addition, the material chosen must have a high ionic conductivity and a near-zero electronic conductivity over a wide range of temperatures and oxygen partial pressures. This shortens the list of suitable materials significantly.

Some other materials (e.g. Bi_2O_3 and CeO_2) show higher oxygen ion conductivity then YSZ, but are less stable. Stability at low oxygen partial pressures (as found at the anode of a SOFC) and on thermal cycling are both critical to cell performance and therefore to material suitability. Sahibzada et al. [23] made some progress in using gadolinium to stabilise ceria at low oxygen concentrations, however.

The main drawback of YSZ is the high temperature requirement. Materials with good oxygen ion conductivity at lower temperatures have been researched, resulting in the development of a lanthanum strontium gallate mangnesite (LSGM) system. This LSGM material is a good oxygen ion conductor, and, at 800 °C, gives performance comparable to that of YSZ at 1000 °C [24,25].

More recently, GDC (gadolinia-doped ceria) electrolytes have been used [26]. This has the problem that GDC is a mixed electronic and ionic conductor, so the electronic conductivity needs to be blocked somehow for successful operation. The use of bilayer electrolytes has been investigated for this purpose [27,28]. Yamaguchi et al. [27] used scandia-stabilised zirconia as the interlayer, forming the bilayer by a cosintering technique. This yielded stable performance and a 60% increase in power density as compared to their cell without a bilayer electrolyte. Ahn et al. [28] used ESB ($[(Bi_2O_3)_{1-x}(Er_2O_3)_x]$–Ag) as the second part of the bilayer with GDC. This gave a significant improvement in both resistance (40% reduction) and power density (93% increase) as compared to a single GDC layer electrolyte.

Use of the anode-supported design allows for a thinner electrolyte. This is generally seen to improve performance, but extra care must be taken to avoid the formation of microcracks, and to ensure the layer is entirely gas tight [29].

The anode: The main requirements for the mSOFC anode material are:

- High porosity (for transport of gases)
- Ionic and electronic conductivity
- Stability/durability

The oxidation of fuel for current generation occurs at the anode, so the anode's role is to facilitate this reaction as much as possible. This reaction occurs at the three-phase boundary, where electrode, reactants and electrolyte meet, making porosity and mixed conduction vital for performance. Experiments have been performed to test various pore-formers (for example in the work of Haslam et al. [30]) and a porosity of around 50% seems preferable, with strength becoming an issue at higher porosities.

The "standard" nickel–YSZ cermet works well in this respect due to the electronic conduction of the metal and ionic conduction of the ceramic, so long as interconnectivity of the two phases is ensured. The YSZ also inhibits sintering of the nickel particles, which would degrade cell performance.

The presence of YSZ in both the anode and the electrolyte helps to match thermal expansion coefficients, reducing cracking on thermal cycling. Adding a dopant such as ceria [31] helps to improve performance on temperature and RedOx cycling, and careful control of YSZ particle size and anode porosity [32,33] also helps to improve the stability under RedOx conditions.

The cathode: The main requirements for the mSOFC cathode material are the same as for the anode. Cathode optimisation is critical as the oxygen reaction occurring here is often the rate limiting factor, so various materials and layered designs are under research [18,34,35]. The use of interlayers has become very popular in recent research, with such a layer often being placed between the cathode and electrolyte to inhibit unwanted chemical reactions [26,36].

The traditional material, LSM, is a poor mixed conductor, however, so other materials seem likely to replace it as the standard. More recently, an LSM/YSZ mixture has been used. With this composite, a 50:50 mass ratio and a fairly large (d_{90} of 26.0 μm) LSM grain size in the outer cathode collection layer has been found to be optimal [37]. Examples of other such materials for replacing LSM include mixed conducting perovskites, lanthanum strontium ferrite and lanthanum strontium cobalite [38,39]. Alongside the popular manganite-based perovskites, those containing iron and cobalt have also been investigated [36]. Mai et al. found that $La_{1-x-y}Sr_xCo_{0.2}Fe_{0.8}O_{3-\delta}$ cathodes gave much better current densities that those based on manganite, with a high strontium content giving a positive effect (increasing current density at 0.7 V by approximately 100%) [36]. The recent review of Sun et al. [40] examines material and microstructure options in more detail.

3. Reported performance

There are three main aspects of fuel cell performance when looking at power generation. These are power density (areal or volumetric), efficiency and durability. The definition of efficiency remains controversial, so will not be addressed here. Fuel utilisation is a major factor to be considered when looking at efficiency, however, and this will be discussed in Section 4. Reported areal power densities ($W\,cm^{-2}$) achieved in the literature in the last few years are given in Table 2, and durability will be discussed in Section 4.

The following standard abbreviations are used in Table 2:

GDC: gadolinia-doped ceria
LSCF: lanthanum ferrite perovskite (La–Sr–Co–Fe–O)
LSM: lanthanum strontium manganite
NiO: nickel oxide
YSZ: yttria-stabilised zirconia

It should be noted that the vast majority of recent work on mSOFCs uses the anode-supported design; all of the cells listed in Table 2 are anode supported. Only the main material for the major cell components are listed in this table—details of binders and pore-formers used, as well as further information on how the cells were produced, can be found in the referenced papers. All the anodes listed here are nickel cermets, with a variety of dopants, particle sizes and pore-formers. A wider range of electrolyte and cathode materials are represented.

4. Key aspects

Solid oxide fuel cells are complex systems, with performance determined by the interplay of many different physical and chemical processes. Particular key issues have been identified by researchers, however, and summaries of their findings are given below.

4.1. Durability

There are two separate aspects of durability; firstly the tolerance of the cell to fuels other than pure hydrogen, and secondly the level of degradation the cell suffers on thermal and RedOx cycling.

4.1.1. Operation on hydrocarbon fuels

Unlike Polymer Electrolyte Membrane fuel cells, SOFCs operate at a high enough temperature for endothermic reforming of hydrocarbons to occur on the anode surface. SOFCs can therefore use hydrocarbons as fuel [41,42]. Running directly on hydrocarbon fuels, however, results in carbon deposition on the anode surface which impairs cell performance. The heat output from SOFCs can be used, along with a catalyst, to pre-reform the hydrocarbon before it enters the cell [43–46], or for internal steam reforming if steam is co-fed to the cell along with the hydrocarbon fuel. Bessler [47] compares and contrasts direct oxidation and internal reforming. Pre-reforming has been shown to reduce carbon deposition, but the catalysts used are expensive, with that developed by Chen et al. [44] being 1% platinum by weight.

There are three known techniques for minimising carbon deposition at the anode for direct hydrocarbon utilisation. These are using various anode-dopant combinations, such as Ni/YSZ with molybdenum or ceria [48–50] (or indeed avoiding the use of nickel entirely [51]), using catalyst or barrier layers [52–54] and modifying the anode reduction technique [42,55]. The same principles apply to any geometry of SOFC.

The use of various anode materials and dopants is discussed by Jiang and Chan [56] who conclude that using materials with

Table 2
Single cell mSOFC performance as reported in the literature.

Ref.	Year	Power density ($W\,cm^{-2}$)	Temp. (°C)	Cell diameter (mm)	Anode material	Electrolyte material	Cathode material	Fuel	Fuel utilisation (%)
Suzuki et al. [33]	2009	1.1	600	1.9	NiO-Sc-stabilised zirconia (ScSZ), Ce-doped zirconia (10Sc1CeSZ)	Zirconia-based: 10Sc1CeSZ	LSCF-GDC	H_2	~3.4[a]
Sammes et al. [106]	2009	1.02	570	0.8	NiO-GDC	GDC	LSCF-GDC	H_2	~54[a]
Suzuki et al. [26]	2007	1.017	550	0.8	NiO-GDC	GDC	LSCF	H_2	~56[a]
Jin et al. [74]	2007	0.645–0.848	800	8	NiO-YSZ	YSZ	LSM	H_2	~4[a]
Sammes et al. [106]	2009	0.84	550	0.8	NiO-GDC	GDC	LSCF-GDC	H_2	~43[a]
Lee and Kendall [73]	2007	0.7	850	2.5	NiO-YSZ	YSZ	LSM/YSZ[b]	CH_4	
Suzuki et al. [26]	2007	0.628	500	0.8	NiO-GDC	GDC	LSCF	H_2	~33[a]
Suzuki et al. [33]	2009	0.5	550	1.9	NiO-Sc-stabilised zirconia (ScSZ), Ce-doped zirconia (10Sc1CeSZ)	Zirconia-based: 10Sc1CeSZ	LSCF-GDC	H_2	~2[a]
Dhir and Kendall [42]	2008	0.425	850	2.3	NiO-YSZ	YSZ	LSM	CH_4	79[a]
Galloway and Sammes [71]	2007	0.3	450	1.8	NiO-GDC	GDC	LSCF-GDC	H_2	~30
Suzuki et al. [26]	2007	0.273	450	0.8	NiO-GDC	GDC	LSCF	H_2	~14[a]
Akhtar et al. [72]	2009	0.122	750	2	NiO-YSZ	YSZ	LSM	CH_4	<11.4

[a] Values calculated from data given in paper; approximate only, simplistic assumptions made *methods given in Appendix*.
[b] Two layers with different LSMs: $La_{0.5}Sr_{0.5}MnO_3$ and $La_{0.82}Sr_{0.18}MnO_3$.

mixed ionic and electronic conductivity helps to improve operation on both hydrogen and methane. Zhang et al. [49] conclude that, "Although the carbon deposition was not suppressed absolutely [by the use of samaria-doped ceria additions to the Ni/YSZ anode], some deposited carbon was beneficial for performance improvement". Dhir and Kendall [42], Mallon and Kendall [55] and Latz et al. [57] similarly observed improved performance when using methane fuel instead of hydrogen in cells modified to avoid problematic carbon deposition. The drawback of nickel-based anodes is that nickel catalyses carbon formation when the ratio of steam to carbon on the anode side is low. This deposited carbon can severely degrade cell performance. Materials including electronically conductive perovskites and copper based cermets have been suggested as alternatives [51]. McIntosh et al. [58,59] investigated the use of Cu/CeO_2/YSZ anodes, and found that using precious metal catalysts helps to increase the OCV of the cell when hydrocarbon fuels are used.

Using catalyst and barrier layers to suppress coke formation has also been investigated. Inert layers work as physical barriers, modifying the ratios of reactants and products present at the anode surface [41]. The increased ratio of water and CO_2 to hydrocarbon fuel at the anode surface shifts the equilibrium position away from coking reactions. Catalytic layers, by contrast, use the chemical properties of the layer to promote partial oxidation reactions of the fuel that do not lead to carbon deposition [53]. To quote Klein et al. [60], this reduces coking of the anode because "the greater part of the reforming reaction occurs in the catalyst layer, and therefore, most of the hydrocarbon species are eliminated before the fuel has reached the anode." The catalyst chosen must not cause coking itself, so materials such as chromite and ceria are recommended [60].

Lin et al. [52] used an inert, porous layer as a barrier between the anode and fuel stream. Their results "demonstrate that diffusion barrier layers increase the stable operating parameter range of Ni-YSZ anode-supported SOFCs operating directly with methane". At 800 °C, they found that use of such a barrier layer reduced the current density required to avoid coke formation three-fold. They agree that the cause is the barrier layer increasing the product (H_2, H_2O, CO, and CO_2) concentration and decreasing the methane concentration in the anode. Zhan and Barnett [53] looked at the use of a ruthenium-ceria catalyst layer. This was found to enable partial oxidation of propane at temperatures above 500 °C without carbon formation at the anode (a propane–air mixture was used). This is a marked improvement as carbon deposition would be expected at temperatures of up to 773 °C for this gas composition. Resultant gas diffusion limitations were found to limit the high temperature performance, however. Yoon et al. [54] used a coating layer of samaria-doped ceria in the anode pores to improve cell performance with methane fuel. This was also shown to reduce carbon deposition and nickel sintering, giving over 500 h of operation without significant degradation.

Dhir and Kendall [42] investigated the effect of anode reduction technique on cell performance with methane fuel. They found that reduction at a constant, reasonably low (650 °C), temperature was optimal. This is thought to produce fine, evenly sized nickel particles. The conductivity is relatively low, as the connectivity of the nickel particles is not high. Graphitic carbon deposition is hypothesised to aid conductivity by producing conducting "bridges" between the particles, increasing connectivity and so conductivity (Fig. 2, courtesy of Dr. Aman Dhir). The performance was notably better for methane than for hydrogen fuel (9% increase in current density when CH_4 was used instead of H_2 at 0.5 V and 850 °C [42]); this was attributed to carbon deposition from the methane obstructing the sintering of nickel particles and so helping to preserve the anode microstructure during use, as well as the afore-mentioned bridging properties. This performance-enhancing effect is not permanent, as further carbon deposition will eventually damage the anode substrate.

McIntosh et al. [61] had previously observed similar improvements in performance due to hydrocarbon deposits, in their case using copper instead of nickel as the metallic component of the anode. They likewise concluded that this was due to the carbon deposits improving connectivity and so conductivity of the metallic anode components. Performance improved most dramatically when the metal made up less than 20% of the anode by weight.

Use of a large enough flux of O^{2-} ions through the electrolyte to remove the carbon as the deposits form on Ni-based anodes has also been investigated, with some success [62,63]. Additionally, Kendall et al. [64] showed that diluting methane with carbon dioxide or inert gas allowed for more stable operation by shifting the equilibrium point of the carbon deposition reaction. For methane fuel, they found that such a mixture could be fed directly into the cell, with the optimal mixture being around 30% methane, 70% carbon dioxide.

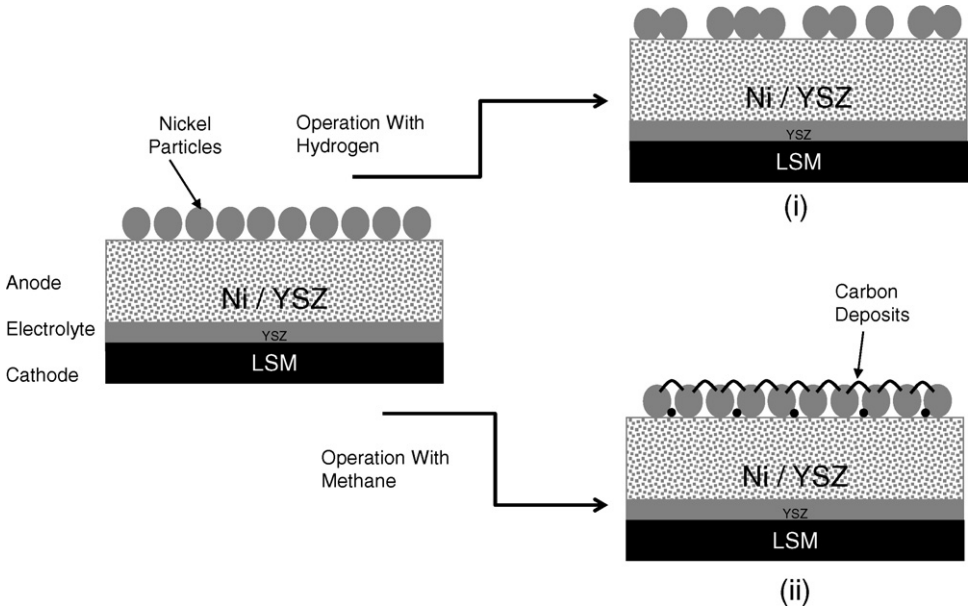

Fig. 2. Proposed mSOFC anode structure following constant temperature reduction and then operation on (i) hydrogen and (ii) methane (operation at 850 °C).

4.1.2. Thermal and RedOx cycling

During use, mSOFCs are subjected to cycling of both temperature and electrochemical conditions. These processes can both cause microstructural defects in the cell, impairing cell performance. Cycling of SOFCs damages the cells in two distinct ways.

Firstly, the temperature gradient leads to degradation during thermal cycling, due to varying expansion coefficients between components, with microcracks opening up in the anode [65]. These separate the nickel particles, and so increase resistance, giving a corresponding worsening of performance. This was investigated in detail in the REAL SOFC project [66] (see Kendall's review [10] for a more detailed summary), and a relationship similar to those for mechanical fatigue was established.

Lawlor et al. [67] give a summary of summary of observed thermal cycling capabilities of mSOFCs. Du et al. [68] found single mSOFCs to have very good thermal shock resistance, withstanding temperature changes of 550 °C min^{-1}. They also found that stacks could be started up within 5 min, and could withstand over 50 thermal cycles. With single cells, 0% power degradation was seen after 150–338 cycles. The work of Bujalski et al. [69] showed that their micro-tubular cells used could be comfortably raised to their operating temperature of around 800 °C within 10 s, and also cooled rapidly. This allows many hundreds of cycles to be performed in quick succession. They also found that such rapid cooling (falling to below 300 °C in a matter of seconds) increased the RedOx deterioration resistance of the nickel cermet anode, as the temperature quickly became too low for any such oxidation to occur. The temperature was cycled up and down every 10 min to 800 °C from room temperature. The first few cycles were found to be the most damaging, with current dropping by about 1% per cycle. The deterioration slowed down after that, however.

Secondly, RedOx cycling (where the fuel flow is interrupted then restarted, at constant temperature) is shown to lead to increased damage [70] due to the nickel in the anode oxidising then reducing. This repeated expansion and contraction extends existing microcracks. As mentioned above, if the cell is cooled rapidly to below the temperature at which this deleterious reaction can occur, there is little time for the nickel to oxidise, improving RedOx durability. This is in opposition to the gentle temperature gradients preferred for thermal cycling durability. As such, the choice of heating or cooling rate must be a trade-off between these two concerns [10], leading to the existence of an optimal temperature ramp rate for a given mSOFC.

4.2. Fuel utilisation

Using a high fuel flow rate maximises the electrical performance at the expense of fuel utilisation. This gives a biased view of efficiency as hydrogen wastage is often ignored.

This point is well addressed by Galloway and Sammes [71] and is discussed in more detail in "High-Temperature Solid Oxide Fuel Cells: Fundamentals, Design and Applications" by Kendall and Singhal [6]. The definition of fuel utilisation (U_f) is not simple, however. Two potential definitions are discussed in the paper of Akhtar et al. [72]. In brief, the two options are:

$$U_f = \frac{1}{nFv} \quad \text{(i)}$$

where I, n, v and F are the current (A) drawn from the cell at peak power density, the number of electrons transferred in the reaction between hydrogen and oxygen ($n = 2$ for hydrogen), the flow rate of fuel (moles/s) and Faraday's constant, respectively (as used by Galloway and Sammes [71] amongst others).

$$U_f = 1 - \frac{m_{out} \times \Delta h_{out}}{m_{in} \times \Delta h_{in}} \quad \text{(ii)}$$

where m_{out} and m_{in} are the mass flow rates of fuel leaving and entering the cell (kg s^{-1}), respectively, and Δh_{in} and Δh_{out} are the specific enthalpies associated with completely oxidising the inlet and outlet fuel (kJ kg^{-1}), respectively.

There are advantages and disadvantages of each method. The first only considers the amount of fuel converted into externally useable electrical energy; the effective utilisation calculated will therefore be slightly smaller than the amount of hydrogen reacted due to various losses incurred in the cell, with the current collection efficiency having a significant effect. The large amounts of thermal energy released by any burning of the fuel at the outlet are also ignored. It has the advantage, however, that it is easily calculable.

The second equation will account for thermal and other losses, but is less intuitively obvious. In addition, the thermal energy may

not be useful (either in combined heat and power applications, or in keeping the cell at the high temperature required for operation), so accounting for this energy is not necessarily helpful in discussions of efficiency. For these reasons, (i) is generally more popular, and is the definition of choice here (as used in Table 2).

With hydrocarbons, it has been found [73] that increasing the fuel flow rate (thereby decreasing the utilisation) can have a negative impact on cell performance beyond a certain point due to increasing carbon deposition on the anode. Optimal performance is therefore seen at a higher percentage fuel utilisation when the fuel contains carbon. The exception here is the single-chamber mSOFC of Akhtar et al. [72]; the fuel and oxidant mix inside a single chamber enclosing the mSOFC. As such, a significant amount of the fuel will not pass near the anode, leading to a lower fuel utilisation. McIntosh and Gorte's theoretical discussion [51] suggests that higher percentages of fuel conversion will give better results when a hydrocarbon is used than when hydrogen is used, everything else being equal.

Suzuki et al. [33] found that increasing linear fuel velocity of hydrogen improved performance up to a point, but that gas diffusion then became the limiting factor. Microstructural porosity becomes the differentiating factor.

4.3. Porosity

Electrode porosity is essential to maximise the area of the three-phase boundary, however there must be an upper limit on optimal porosity for conductivity and structural stability to remain sufficiently high. Jin et al. [74] found that porosity should be less than 55% to avoid raising the resistivity of the anode excessively. They also point out that pore size is crucial, with larger pores being detrimental to mechanical strength. Suzuki et al. [33] investigated anode microstructure, concluding that, "the electrochemical performance of the cell was extensively improved when the size of constituent particles was reduced so as to yield a highly porous microstructure". They found the best performance when the Ni particles of the anode were smaller than 100 nm across.

The cells with the best performance recorded in the literature to date (Suzuki et al. [33]) had a porosity of 54% (before reduction). This represents a balance between porosity to aid gas flow and continuity of material to aid conductivity.

The effects of volume percentages of pore-formers used [75] and the type of material used as the pore-former [30,74,76] have been investigated.

Tubes with higher porosities are generally mechanically weaker; Roy et al. [75] quantified this weakening for three pore-former volume percentages (40%, 50% and 60%), seeing a drop of approximately 26% in average burst strength for each 10% volumetric increment of pore-former. This average burst strength was 11.7 ± 7.5MPa for the test tubes with 60% pore-former by volume; this should be sufficient in most cases, but this weakening effect of increased porosity must be a consideration where hard-wearing cells are required.

Jin et al. [74] investigated the use of flour as a pore-former, alongside the more standard graphite. The flour showed more significant shrinkage on sintering, leading to a number of larger pores big enough to be problematic in terms of cell strength. Flour decomposes by a violent burning reaction, and this led to an uneven pore distribution, as well as the size variation mentioned. The graphite pore-former was found to be preferable due to the even spread of smaller pores giving good gas permeability and a large surface area without overly compromising cell strength. Hu et al. [77] had some success developing a composite pore-former comprised of flour and activated carbon. Wang et al. [76] found magnesium oxide to be preferable as a pore-former in their silver-impregnated $Ce_{0.8}Sm_{0.2}O_{1.9}$ anode.

4.4. Current collection

Overall cell resistance increases with increasing Ohmic resistance, causing the electrical performance to decrease. The length and resistance of the current collection path is therefore critical, especially as mSOFCs generally have a much longer current path than other SOFCs. One experimental set-up [74] showed a 24% decrease in power density when the distance of the cell from the anode current collection point was increased by a factor of seven.

Whilst collecting the anode current along the whole electrode length would be ideal, the small tube size makes this a difficult feat of engineering. Cui et al. [78] found that having a current collection point at both the inlet and the outlet of the cell has a significant positive impact on cell performance as opposed to a single collection point. Suzuki et al. found that using this "double terminal" current collection method reduced the efficiency loss two- to four-fold as compared to single terminal collection [79] (these results were confirmed by in-house experimentation [80]). Decreasing electrode length and increasing its conductivity were also shown to improve performance here. The cell length again emerged as a crucial factor in later work of Suzuki et al. [81], with a 7% loss in performance due to current collection efficiency seen for cells above 1 cm in length.

Zhu and Kee [82] developed a mathematical model to assist with current collection design for anode-supported tubular SOFCs. Resistance and placement of current collection materials were seen to have a notable effect on local temperature and species distributions, as well as on overall performance (fuel utilisation and power density being key examples). They found that more current collection points should be used on the cathode than on the anode. These principles will also apply to the micro-tubular cells.

It has been observed that minimising the cell length maximises the performance per unit area; the length of the current collection path is thought to be the responsible factor [74].

5. Single cells: ongoing developments

As previously mentioned, the power density of mSOFCs depends on the inverse of the cell diameter. Making yet narrower tubes is therefore a promising line of research. Work has been done on YSZ hollow fibre tubes, with external diameters of around only 1.6 mm, and sub-millimetre internal diameters [2,83,84]. The fabrication processes were carefully controlled to give open and interconnected pores on the external and internal surfaces, giving a high surface area for the electrodes, and a thin dense gas-tight central layer giving low Ohmic resistance. There is a great deal of ongoing research in Japan looking at micro-tubes of sub-millimetre diameter to obtain higher power densities [26,85]. Dual-layer hollow fibre cells have also been fabricated [86] with maximum power densities of $0.042\,W\,cm^{-2}$ and $0.08\,W\,cm^{-2}$ at 450 °C and 550 °C, respectively. The concept has thus been demonstrated, and continued optimisation of manufacturing processes and microstructural control will improve performance further.

Work has also been done to improve the RedOx stability of anode materials [87]. By dispersing the nickel more finely in the anode structure, less should be required to give the same performance. This means there is less nickel available to be oxidised and then re-reduced, decreasing the damage done by this process. Ouweltjes et al. [87] observed a drop in current density at 0.7 V of 10% after 50 RedOx cycles and 23% after 100 with their cells utilising highly dispersed nickel.

The development of stack designs is also critical to the commercial adoption of mSOFCs. The power provided by an individual cell is too small for most applications so intensive research into

stack design is receiving a great deal of interest, both for modelling and experimental work [67,88–91]. The following section explores stack designs and modelling achievements in the literature.

6. Stack designs

The first mSOFC stack designs [11,12] consisted of modular combinations of sets of cells in individual racks used to build up to the required power output. For the 1000-cell stack, the cells were arranged in racks of 40. This modular arrangement helps to facilitate even gas distribution throughout the stack—each rack had a tubular gas distribution manifold to help ensure uniformity [12]. In this instance, the tubes were connected in parallel and the racks in series to provide the voltage and current desired. Although this stack produced only 0.082 W cm^{-2} at 850 °C, this served as proof of concept. This arrangement has another advantage in that the modules can be removed and replaced individually in case of failure, without losing the entire stack; this feature is popular in more recent designs.

6.1. The use of modelling

The hydrogen fuel cell provides a complex modelling challenge due to the number of different physical processes involved. These include heat and mass transfer by various mechanisms, chemical and electrochemical interactions, macro-scale fluid dynamics and micro-scale molecular interactions. In addition to these issues, certain fundamentals of the electrochemical reaction mechanisms in solid oxide fuel cells (SOFCs) are not yet fully understood.

Many models in the literature have a strong focus on one particular aspect, with fewer actually incorporating all aspects as would be required for a model aimed to have predictive power. Nonetheless, these models all provide valuable insight as detailed in the following text. Reviews such as that of Kakac et al. [92] give an overview of the key assumptions and equations used in SOFC modelling to date. Here, results are summarised, not the modelling techniques.

As discussed in Lawlor's review [67], computational modelling has greatly helped understanding of transport in stacks, amongst other phenomena. Lockett et al. [88] describe the results from a single mSOFC alongside their work on thermal distributions and heat use in a stack of twenty cells. The main problem for single cells highlighted by this work is that the temperature varies significantly from the optimum even along a relatively short active length (25 mm). Despite this temperature variation, Cui and Cheng [93] found that the main source of thermal stress in mSOFCs is the mismatch of material expansion coefficients, not thermal gradients within each layer. They conclude that matching coefficients of thermal expansion is the most important factor in ensuring cell reliability.

Serincan et al. [94] looked at the effects of operating conditions on cell performance, and more specifically at the temperature dependence of current leaks. They conclude that current leakage does not have a significant effect below 500 °C; unfortunately this is below the current range of most SOFCs. An increase in temperature results in better cell performance overall, however, due to increased catalytic activity and ionic conductivity. They also note that a change in pressure has more effect at the cathode side than at the anode side due to the slow reaction kinetics of the cathode.

Izzo et al. [95] highlight the importance of diffusion within the anode layer for cell performance. The gas and voltage distributions along the tube were found to vary significantly when a diffusive anode layer was incorporated into their model.

Cui et al. [78] investigated the efficacy of different current collecting methods with varying tube length for mSOFCs. They found collecting current from the anode at both the inlet and the outlet of the cell more efficient than from either individually by a factor of ~2–6, in good agreement with experiment [79]. Collecting current at the outlet only does however give a much more uniform electrochemical reaction distribution in the cell.

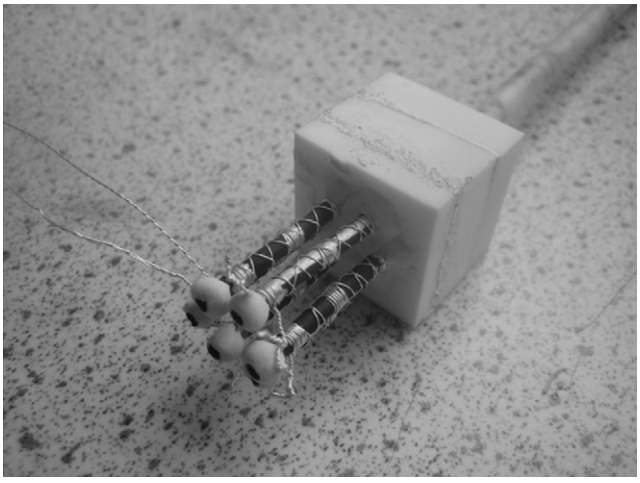

Fig. 3. mSOFC stack designed, built and tested at the University of Birmingham.

More recent modelling work by Funahashi et al. [96] examined a module-type mSOFC stack as discussed in more detail in the following section. Air flow, Joule heat and temperature distribution were the main focuses. A temperature difference of 100 °C across the 1 cm^3 stack was a striking illustration of the necessity of optimising the design to give an even temperature distribution. Thinner tubular cells were found to lead to lower air pressure loss in the cathode matrix. Their simulation confirmed that the Joule heat caused by the anode tube and cathode matrix resistances was negligible as compared to that from the internal cell resistance (smaller by a factor of 1000). As such, this can be safely ignored for the purposes of most simulations.

As yet, there is no off-the-shelf stack design model available, and single cell models with good predictive power are notably lacking. Nonetheless, this can be a very useful design tool.

6.2. A simple in-house experimental stack

A stack of six mSOFCs was produced [80] by cementing six tubes made according to in-house techniques (detailed in [42,97]) to a fuel injection manifold, as shown in Fig. 3. The circular symmetry of the cells around the fuel inlet should ensure an equal flow rate of fuel to each cell, which is essential for effective stack operation. The cells are connected in series by silver wire, enabling a flow of electrons from the anode of one cell to the cathode of the next. The simplicity of this design, with clearly visible interconnections, seals, inlets and outlets, facilitates basic stack performance characterisation.

Current–voltage (IV) characterisation was performed on the stack, and on a single cell made in the same way. A Solartron™ analytical 1400 Cell Test System (connected to a computer where purpose-built programmes were designed using Cell Test™ v 5.2.0 software) was used. The stack was tested at 750 °C with a fuel (hydrogen) flow rate of 100 ml min^{-1}. The stack was heated at 75 °C min^{-1} and loaded at 1 A once the operating temperature was reached. A constant current was drawn for 3 h before a current ramp was applied in order to produce a power curve. The single cell was tested in the same way for comparison purposes.

The results given in Fig. 4, below, show that the voltage of the stack was very close to that of a single cell multiplied by six. This is the expected result for a correctly operating stack, indicating that

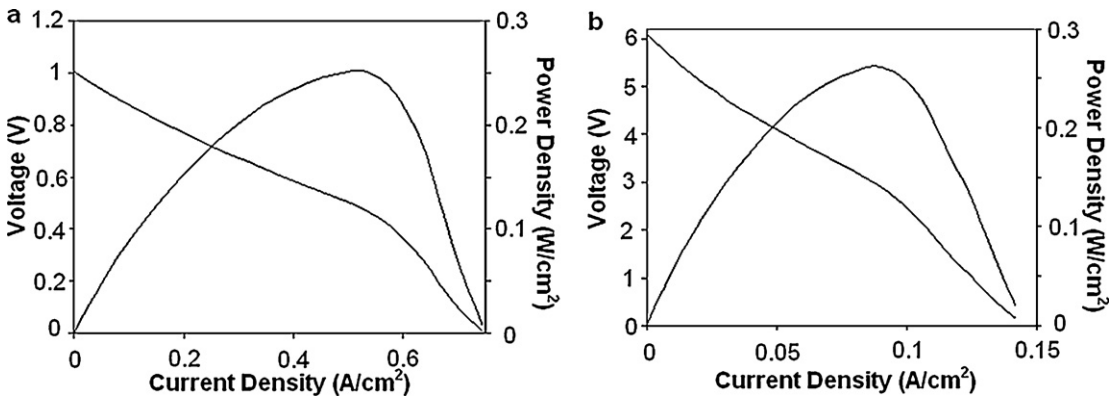

Fig. 4. Graphs of individual cell (a) and stack (b) performance, showing both power density and voltage against current density.

the fuel delivery to each cell is equal, and that the outputs of the cells within the stack are well matched. Both the stack and single cell show a peak power density close to 0.25 W cm^{-2} (each cell having an area of ~1.96 cm^2; 11.76 cm^2 for the stack), although this peak occurs at a far lower current density in the stack, due to the presence of six cells in series. To generate a larger current, more cells should be connected in parallel. Notably the OCVs of the cell and stack were below 1.1 V, hence lower than desired, but the particular cell weakness leading to this was not identified.

This work also highlighted the importance of obtaining very similar performance from each of the cells in a stack [80]. If the electrical power of each of the cells is not well matched, the performance degrades far more quickly than normal. As the cells are connected in series, the same current is applied to each. Any weaker cells in the stack would effectively be working harder to maintain the same current output as the higher performing cells, leading to a higher rate of degradation. Eventually, the weakest cell's performance would degrade to a point where it was unable to produce the required number of electrons to maintain the current being drawn. It would then become an additional load on the other cells, with a similar effect to connecting a resistor in series. The increased load on the other cells would increase their degradation rate, ultimately leading to stack failure. The stack is therefore only as good as its weakest cell. This reinforces the advantages of opting for modular stack designs, so a small section of a large stack can be removed and replaced as soon as an issue is detected.

6.3. Experimental stacks in the literature

In 2008, Suzuki et al. [91] created an mSOFC stack with a volume of 1 cm^3, which they operated at 500 °C. This gave a maximum power output of 1.5 W. Each module was composed of three cells, held in place by a shaped block of the cathode mixture (as shown in Fig. 5). The stack consisted of three such modules in series. Further testing of this design, but with 0.8 mm diameter tubes replacing the previous 2 mm diameter tubes, was also performed [85]. This gave a power density of 2 W cm^{-3} at an operating temperature of 550 °C.

Yamaguchi, Suzuki et al. [89] also looked at the possibility of using a honeycomb arrangement for an mSOFC stack. This design was postulated for tubular cells in 1999 [98], and the mSOFC version showed a promising volumetric power density (0.6 W cm^{-3} at 600 °C with tube diameter ~1.6 mm). Like the shaped support for the previously mentioned design, the honeycomb was made from the cathode material and metallic interconnects were used.

Funahashi et al. [90] used a magnesium oxide matrix to support their stack design instead of extruded cathode material, and obtained a power density of over 0.6 W cm^{-3} at 500 °C. Sufficient air for the cathode could flow through this MgO matrix. The design was otherwise very similar to that shown in Fig. 5, although the "bundles" were stacked on top of each other instead of side-by-side, giving a more cubic stack. In other work [99], they used a similar design but with the porous matrix made from the cath-

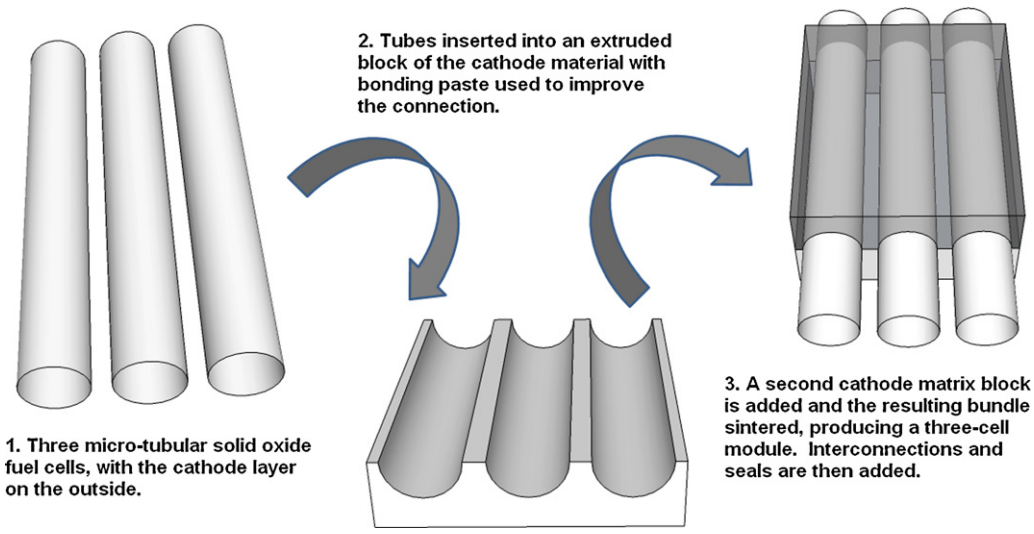

Fig. 5. Sketch of a three-cell module design.

ode material. The effect of tube spacing within such bundles was investigated by Suzuki et al. [9]. They discuss the trade-off between densely packed tubes giving a higher surface area per unit volume and loss in performance due to reduced gas flow and extended current paths. They obtained a power density of 2.5 W cm^{-3} at 550 °C, with a tube diameter of 0.8 mm.

Sammes et al. [100,101] used a similar "planar multicell array" arrangement as for the modules of Suzuki et al. (Fig. 5), and obtained a power of 100 W with 40 cells. The cells they used however were more similar to the older tubular cells, having diameters of 1.32 cm and lengths of 11 cm. As such, the volumetric power density is much lower (~0.13 W cm^{-3} at most). Lee et al. [102] similarly used cells of around 1 cm diameter for their 700 W stack, which consisted of 36 such cells, each of length 20 cm. Again, these 36 cells were arranged into bundles (of six), giving the stack a modular nature.

Du et al. [68] tested NanoDynamics' (later, "ndEnergy") micro-tubular stacks and found very promising results including start-up within 5 min and good thermal cycling characteristics. Other mSOFC stacks have been tested by Crumm [103] Adaptive Materials Inc., but details of both researchers' work are proprietary.

7. Summary

Resistance to thermal and RedOx cycling degradation, fuel utilisation, electrode porosity and current collection have been identified as the four main differentiating factors of fuel cell performance from a cell design viewpoint. A summary of recent developments and the supporting reasoning is given. In terms of stack power densities; the maximum found in the literature was 2.5 W cm^{-3} at 550 °C [9], although balance of plant volumes must be taken into account for industrial applications.

Micro-tubular SOFCs provide an active research area, as demonstrated by the number of papers published in recent years. With objectives such as materials suitable for lower temperatures of operation [104] and better interconnections [105], it promises to remain a productive area in the near future.

Acknowledgements

With thanks to the RCUK and EADS Innovation Works for their sponsorship of Miss K.S. Howe, and also to Dr. A. Dhir for his help and advice.

Appendix A. Calculations of fuel utilisation

The formula used is formula (i) given earlier: $U_f = 1/nF\nu$

The specific information used for each paper listed is given below. For hydrogen, $n = 2$, for methane, $8 \geq n \geq 4$, and $n = 8$ was used to give a minimum utilisation. Numbers in bold are taken straight from the papers. Where no details are given, the fuel is assumed to be an ideal gas at room temperature, with negligible humidification.

Suzuki et al. [33]
Electrolyte area = 0.3 cm^2
Linear fuel velocity: 0.8 m/s
1.9 mm cell diameter
a cross-section of 0.028 cm^2
Current densities from graphs in Fig. 3A and B, and calculated total cell currents:
550 °C – 1.25 A cm^{-2} – 0.375 A
600 °C – 2.2 A cm^{-2} – 0.66 A

Sammes et al. [106]
Effective cell area: 0.13 cm^2
Hydrogen flow rate: 5 ml/min
Current densities from graph in Fig. 11, and calculated total cell currents:
550 °C – 2.4 A cm^{-2} – 0.312 A
570 °C – 3.0 A cm^{-2} – 0.39 A

Suzuki et al. [26]
Effective cell area: 0.13 cm^2
Hydrogen flow rate: 5 ml/min
Current densities at each temperature, and the calculated total cell currents:
550 °C – 3.1 A cm^{-2} – 0.403 A
500 °C – 1.8 A cm^{-2} – 0.234 A
450 °C – 0.8 Acm^{-2} – 0.104 A

Jin et al. [74]
0.31 cm^2 effective cathode area
Current density 1.2 A cm^{-2} – 0.372 A
75 ml/min fuel flow rate, 3% water (so 97% H_2) by volume at 25 °C

Lee and Kendall [73]
Insufficient data given in paper

Dhir and Kendall [42]
1.6 cm^2 active cathode area
Current density 0.85 A cm^{-2} – 1.36 A
3 ml min^{-1} fuel flow rate (methane)

Galloway and Sammes [71]
Fuel utilisation read off graph given in Fig. 8 of [69]

Akhtar et al. [72]
Calculation given in paper

References

[1] D.H. Archer, L. Elikan, R.L. Zahradnik, in: B.S. Baker (Ed.), Hydrocarbon Fuel Cell Technologies, Academic Press, New York, 1965.
[2] D.D. Nicolas, et al., ECS Transactions 25 (2) (2009) 665–672.
[3] U.B. Pal, S.C. Singhal, Journal of the Electrochemical Society 137 (9) (1990) 2937–2941.
[4] A.O. Isenberg, Solid State Ionics 3–4(AUG) (1981) 431–437.
[5] W.J. Dollard, Journal of Power Sources 37 (1–2) (1992) 133–139.
[6] K. Kendall, S.C. Singhal, High-Temperature Solid Oxide Fuel Cells: Fundamentals, Design and Applications, Elsevier Ltd., 2003.
[7] K. Kendall, Proceedings of the International Forum on Fine Ceramics. International Forum on Fine Ceramics, Japan Fine Ceramics Center, Nagoya, 1992.
[8] M. Kendall, Tubular cells: a novel SOFC design, Master's Thesis, Middlesex University, 1993.
[9] T. Suzuki, et al., Journal of Fuel Cell Science and Technology 7 (3) (2010) 5.
[10] K. Kendall, International Journal of Applied Ceramic Technology 7 (1) (2010) 1–9.
[11] M. Prica, T. Alston, K. Kendall, in: U. Stimming, et al. (Eds.), Proceedings of the Fifth International Symposium on Solid Oxide Fuel Cells, Electrochemical Society Inc., Pennington, 1997, pp. 619–625.
[12] T. Alston, et al., Journal of Power Sources 71 (1–2) (1998) 271–274.
[13] K. Kendall, M. Prica, 1st European SOFC Forum, Luzern, Switzerland, 1994.
[14] X.Y. Tan, et al., Science in China Series B—Chemistry 51 (9) (2008) 808–812.
[15] H. Luebbe, et al., 11th Electroceramics Conference 2008, Elsevier Science Bv, Manchester, England, 2008.
[16] Y. Liu, et al., Journal of Power Sources 174 (1) (2007) 95–102.
[17] M. Liu, et al., Journal of Power Sources 182 (2) (2008) 585–588.
[18] S.Q. Zhang, et al., International Journal of Hydrogen Energy 34 (18) (2009) 7789–7794.
[19] M. Liu, et al., Journal of Power Sources 180 (1) (2008) 215–220.
[20] Z. Liang, Coextrusion of multilayer tubes, Ph.D., University of Birmingham, 1999 (Chapter 8).
[21] A.J. Jacobson, Chemistry of Materials 22 (3) (2010) 660–674.
[22] Y. Mizutani, Conference of the NATO-Advanced-Study-Institute on Mini-Micro Fuel Cells—Fundamentals and Applications, Springer, Cesme Izmir, Turkey, 2007.
[23] M. Sahibzada, et al., 5th International Symposium on Solid Oxide Fuel Cells (SOFC-V), Electrochemical Society Inc., Aachen, Germany, 1997.
[24] M. Feng, et al., Journal of Power Sources 63 (1) (1996) 47–51.
[25] T. Ishihara, H. Matsuda, Y. Takita, Journal of the American Chemical Society 116 (9) (1994) 3801–3803.
[26] T. Suzuki, et al., Electrochemical and Solid State Letters 10 (8) (2007) A177–A179.
[27] T. Yamaguchi, et al., Journal of the Electrochemical Society 155 (4) (2008) B423–B426.
[28] J.S. Ahn, et al., Electrochemistry Communications 11 (7) (2009) 1504–1507.
[29] Y.H. Du, N.M. Sammes, Journal of Power Sources 136 (1) (2004) 66–71.
[30] J.J. Haslam, et al., 102nd Annual Meeting of the American-Ceramic-Society, Blackwell Publishing Inc., St Louis, MO, 2000.

[31] J. Larminie, A. Dicks, Fuel Cell Systems Explained, Second ed., Wiley, 2003, pp. 210–212.
[32] M. Pihlatie, T. Ramos, A. Kaiser, Journal of Power Sources 193 (1) (2009) 322–330.
[33] T. Suzuki, et al., Science 325 (5942) (2009) 852–855.
[34] K. Tomida, et al., Electrochemistry 77 (10) (2009) 865–875.
[35] R.M. Belardi, et al., Materia-Rio De Janeiro 13 (3) (2008) 522–532.
[36] A. Mai, et al., Solid State Ionics 176 (15–16) (2005) 1341–1350.
[37] V.A.C. Haanappel, et al., Journal of Power Sources 141 (2) (2005) 216–226.
[38] K.K. Hansen, M. Sogaard, M. Mogensen, Electrochemical and Solid State Letters 10 (8) (2007) B119–B121.
[39] P. Han, et al., EPRI/GRI Fuel Cell Workshop on Fuel Cell Technology R&D, New Orleans, LA, 1993.
[40] C.W. Sun, R. Hui, J. Roller, Journal of Solid State Electrochemistry 14 (7) (2010) 1125–1144.
[41] Y. Lin, et al., Solid State Ionics 176 (23–24) (2005) 1827–1835.
[42] A. Dhir, K. Kendall, 10th Grove Fuel Cell Symposium, Elsevier Science Bv, London, England, 2007.
[43] N Laosiripojana, S. Assabumrungrat, Applied Catalysis B—Environmental 66 (1–2) (2006) 29–39.
[44] F.Z. Chen, et al., Solid State Ionics 166 (3–4) (2004) 269–273.
[45] C. Finnerty, et al., Journal of Power Sources 86 (1–2) (2000) 459–463.
[46] J. Zheng, J.J. Strohm, C. Song, Fuel Processing Technology 89 (4) (2008) 440–448.
[47] W.G. Bessler, 8th European Solid Oxide Fuel Cell Forum, Fuel Cell Forum, Lucerne, Switzerland, 2008.
[48] W. Zhu, et al., Journal of Power Sources 160 (2) (2006) 897–902.
[49] L.S. Zhang, et al., Chinese Journal of Chemical Physics 22 (4) (2009) 429–434.
[50] M. Asamoto, et al., Electrochemistry Communications 11 (7) (2009) 1508–1511.
[51] S. McIntosh, R.J. Gorte, Chemical Reviews 104 (10) (2004) 4845–4865.
[52] Y. Lin, Z. Zhan, S.A. Barnett, Journal of Power Sources 158 (2) (2006) 1313–1316.
[53] Z. Zhan, S.A. Barnett, Solid State Ionics 176 (9–10) (2005) 871–879.
[54] S.P. Yoon, et al., 3rd International Conference on Fuel Cell Science, Engineering and Technology, Amer Soc Mechanical Engineers, Ypsilanti, MI, 2005.
[55] C. Mallon, K. Kendall, Journal of Power Sources 145 (2) (2005) 154–160.
[56] S.P. Jiang, S.H. Chan, Journal of Materials Science 39 (14) (2004) 4405–4439.
[57] J. Latz, C. Mallon, K. Kendall, Sixth European Solid Oxide Fuel Cell Forum, Solid Oxide Fuel Cell Forum, Lucerne, Switzerland, 2004.
[58] S. McIntosh, J.M. Vohs, R.J. Gorte, Electrochimica Acta 47 (22–23) (2002) 3815–3821.
[59] S. McIntosh, J.M. Vohs, R.J. Gorte, Journal of the Electrochemical Society 150 (10) (2003) A1305–A1312.
[60] J.M. Klein, S. Georges, Y. Bultel, Journal of the Electrochemical Society 155 (4) (2008) B333–B339.
[61] S. McIntosh, J.M. Vohs, R.J. Gorte, Journal of the Electrochemical Society 150 (4) (2003) A470–A476.
[62] J.A. Liu, S.A. Barnett, Solid State Ionics 158 (1–2) (2003) 11–16.
[63] E.P. Murray, S.A. Barnett, in: S.C. Singhal, M. Dokiya (Eds.), Solid Oxide Fuel Cells, Electrochemical Society Inc., Pennington, 1999, pp. 1001–1009.
[64] K. Kendall, et al., Journal of Power Sources 106 (1–2) (2002) 323–327.
[65] C.M. Dikwal, W. Bujalski, K. Kendall, Journal of Power Sources 193 (1) (2009) 241–248.
[66] Real-SOFC, Real-SOFC project homepage. Available from: http://www.real-sofc.org/, 2009 (cited 06.10.09).
[67] V. Lawlor, et al., Journal of Power Sources 193 (2) (2009) 387–399.
[68] Y.H. Du, C. Finnerty, J. Jiang, Journal of the Electrochemical Society 155 (9) (2008) B972–B977.
[69] W. Bujalski, C.A. Dikwal, K. Kendall, Journal of Power Sources 171 (1) (2007) 96–100.
[70] C.M. Dikwal, W. Bujalski, K. Kendall, 10th Grove Fuel Cell Symposium, Elsevier Science Bv, London, England, 2007.
[71] K.V. Galloway, N.M. Sammes, Journal of the Electrochemical Society 156 (4) (2009) B526–B531.
[72] N. Akhtar, et al., Journal of Power Sources 193 (1) (2009) 39–48.
[73] T.J Lee, K. Kendall, 10th Grove Fuel Cell Symposium, Elsevier Science Bv, London, England, 2007.
[74] C. Jin, et al., Journal of Membrane Science 341 (1–2) (2009) 233–237.
[75] B.R. Roy, et al., Journal of Power Sources 188 (1) (2009) 220–224.
[76] F.Y. Wang, et al., Journal of Power Sources 185 (2) (2008) 862–866.
[77] J. Hu, et al., Journal of Membrane Science 318 (1–2) (2008) 445–451.
[78] D. Cui, et al., Journal of Power Sources 174 (1) (2007) 246–254.
[79] T. Suzuki, et al., Journal of Power Sources 163 (2) (2007) 737–742.
[80] G. Thompson, Improving the consistency of microtubular solid oxide fuel cells for methane fuelled stacks, Ph.D. Thesis—pending examination, University of Birmingham, 2010.
[81] T. Suzuki, et al., Journal of Power Sources 171 (1) (2007) 92–95.
[82] H.Y. Zhu, R.J. Kee, Journal of Power Sources 169 (2) (2007) 315–326.
[83] F. Dal Grande, et al., Solid State Ionics 180 (11–13) (2009) 800–804.
[84] N. Droushiotis, et al., Solid State Ionics 180 (17–19) (2009) 1091–1099.
[85] T. Suzuki, et al., Journal of the Electrochemical Society 156 (3) (2009) B318–B321.
[86] N. Droushiotis, et al., Electrochemistry Communications 11 (9) (2009) 1799–1802.
[87] J.P. Ouweltjes, et al., Fuel Cells 9 (6) (2009) 873–882.
[88] M. Lockett, M.J.H. Simmons, K. Kendall, 8th Grove Fuel Cell Symposium., Elsevier Science Bv, London, England, 2003.
[89] T. Yamaguchi, et al., Materials Letters 63 (29) (2009) 2577–2580.
[90] Y. Funahashi, et al., Fuel Cells 9 (5) (2009) 711–716.
[91] T. Suzuki, et al., Fuel Cells 8 (6) (2008) 381–384.
[92] S. Kakac, A. Pramuanjaroenkij, X.Y. Zhou, International Journal of Hydrogen Energy 32 (7) (2007) 761–786.
[93] D.A. Cui, M.J. Cheng, Journal of Power Sources 192 (2) (2009) 400–407.
[94] M.F. Serincan, U. Pasaogullari, N.M. Sammes, Journal of Power Sources 192 (2) (2009) 414–422.
[95] J.R. Izzo, A.A. Peracchio, W.K.S. Chiu, Journal of Power Sources 176 (1) (2008) 200–206.
[96] Y. Funahashi, et al., Journal of Fuel Cell Science and Technology 7 (2) (2010) 4.
[97] A. Dhir, Improved microtubular solid oxide fuel cells, Chemical Engineering Ph.D. Thesis, University of Birmingham, Birmingham, 2008.
[98] M. Wetzko, et al., Journal of Power Sources 83 (1–2) (1999) 148–155.
[99] Y. Funahashi, et al., in: K. Eguchi, et al. (Eds.), Solid Oxide Fuel Cells 10, Electrochemical Society Inc., Pennington, 2007, pp. 643–649.
[100] N.M. Sammes, R. Bove, Y.H. Du, Journal of Materials Engineering and Performance 15 (4) (2006) 463–467.
[101] N.M. Sammes, Y. Du, R. Bove, Journal of Power Sources 145 (2) (2005) 428–434.
[102] S.-B. Lee, et al., International Journal of Hydrogen Energy 33 (9) (2008) 2330–2336.
[103] A. Crumm, 2006 Fuel Cell Seminar, Adaptive Materials, Inc., 2006.
[104] A.S. Nesaraj, Journal of Scientific & Industrial Research 69 (3) (2010) 169–176.
[105] N. Shaigan, et al., Journal of Power Sources 195 (6) (2010) 1529–1542.
[106] N. Sammes, et al., 32nd International Conference on Advanced Ceramics and Composites, Amer Ceramic Soc, Daytona Beach, FL, 2008.